Application Note

Cardiovascular Research

Agilent

Trusted Answers

Assessment of Cardiomyocyte Disease Models Using the Agilent xCELLigence CardioECR System

Authors

Xiaoyu Zhang, Jeff Li, and Yama Abassi

Agilent Technologies, Inc.

Abstract

The Agilent xCELLigence RTCA CardioECR system combines simultaneous measurement of field potential signal using extracellular recording (ECR) electrodes as well as contractility and viability using impedance electrodes. The real-time multiplexed evaluation of the functional activity of beating cardiomyocytes using the CardioECR system allows for depicting and recapitulating disease phenotype of cardiomyocytes differentiated from patient-specific induced pluripotent stem cell (PS-iPSC) and investigating their pharmacological responses, which could potentially provide information about underlying disease mechanisms.

Introduction

In 2006, Yamanaka and his colleagues established the first induced pluripotent stem cells (iPSC) from murine fibroblasts via transduction of four specific transcriptional factors. This novel discovery was also translated to human somatic cells and has created a new frontier in the medical field in many respects. The characteristics of iPSCs, including infinite self-renewal and multipotency, allow them to be potentially used in a wide variety of applications, including disease modeling, drug screening, and regenerative therapy.[1,2] It is well established that iPSCs obtained from patients maintain patient-specific genetic lesions, providing a rationale for disease modeling using patient-specific iPSCs (PS-iPSCs).[3,4] Even though primary patient cells have previously been used for studying disease mechanisms, certain cell types such as neurons and cardiomyocytes, are rather difficult to obtain. The scalability of primary diseased cells and the duration of maintaining these cells in culture has also been a hurdle for investigating disease mechanisms. PS-iPSC differentiated target cells provide researchers with a stable, scalable, and physiologically relevant cell source for disease modeling.[5] To date, numerous studies have reported that these target cells can recapitulate disease phenotypes similar to those observed from patients. The pathophysiological cellular phenotypes of genetically heritable heart diseases, such as cardiomyopathies and channelopathies, have been successfully modeled *in vitro* using patient-specific iPSC-derived cardiomyocytes (PS-iPSC-CMs).[6] These model systems are promising tools for understanding disease mechanisms and can potentially be used in drug discovery, personalized medicine, and cardiac liability assessment in specific populations that may carry genetic anomalies.

This application note used the Agilent xCELLigence RTCA CardioECR system (CardioECR system) to compare functional profiles of contractility and electrophysiology between a PS-iPSC-CM disease model and its isogenic control. After identifying baseline phenotypes at the cellular level, this study investigated pharmacological responses of diseased and isogenic cardiomyocytes to compounds with established mechanisms. As a further approach to assessing the responses of the wild type and diseased CM, both cell lines were subjected to electrical stimulation followed by treatment with isoproterenol.

Assay principle

The xCELLigence RTCA CardioECR system is a dual-mode instrument that includes both simultaneous monitoring of hiPSC-CM viability, contraction, and field potential (FP) in real time as well as directed electrical pacing of hiPSC-CMs. It consists of four components, CardioECR control unit (laptop), CardioECR analyzer, CardioECR station, and E-plate CardioECR 48 (CardioECR plate) (Figure 1A). Two sets of electrodes, interdigitated impedance (IMP) micro-electrode arrays as well as two individual field potential electrodes are integrated into the bottom of each well of the CardioECR plate (Figure 1B). Similar to other Agilent xCELLigence platforms, the CardioECR System uses IMP electrodes to measure cellular impedance, which is affected by the number of cells covering the electrode, the morphology of the cells, and the extent of cell attachment. The fast sampling rate of IMP measurement (2 ms) allows for capturing of the temporal rhythmic changes in cell morphology and degree of cell attachment to the plate, which is a hallmark of contraction of cardiomyocytes. Therefore, the physical contraction of cardiomyocytes is monitored and recorded in real time with high temporal resolution. Additionally, the millisecond time resolution can be performed at regular intervals over a prolonged duration of

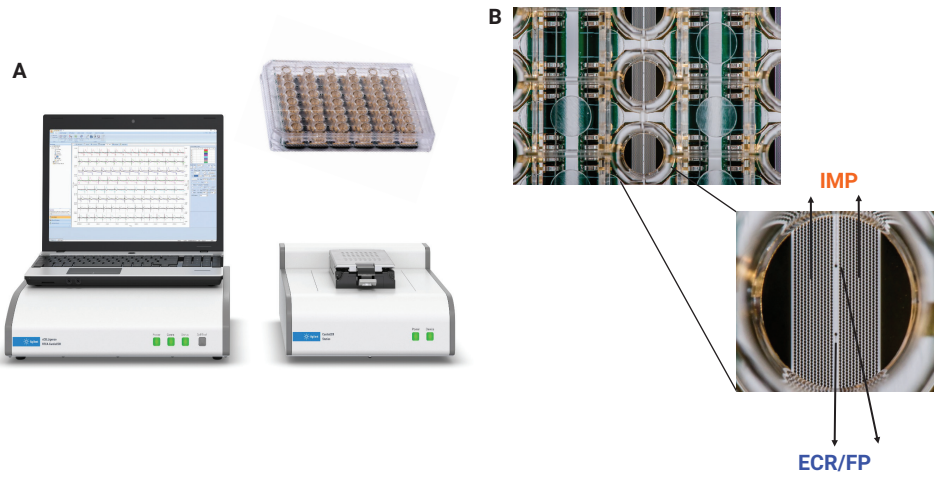

Figure 1. (A) The Agilent xCELLigence RTCA CardioECR system consists of four components: Control unit/laptop, CardioECR analyzer (left), CardioECR station (right), and E-PlateCardioECR 48. (B) A close-up image of E-Plate CardioECR48. Inset: a close-up of the wells reveals the layout of the electrodes, impedance (IMP) electrode assays, and two field potential (FP) electrodes.

time providing beating and viability information of cardiomyocytes in real time. Furthermore, two field potential electrodes are used to measure integrated ion channel activities at a data acquisition rate of 10 kHz simultaneously while IMP recording is taking place via IMP electrodes. A typical workflow of cardiomyocyte assay using CardioECR system is shown in Figure 2.

One of the other critical features of the CardioECR system is its ability to electrically pace cardiomyocytes. During electrical pacing, electrical pulses are directly applied to the cells through the IMP electrodes. For most cardiomyocytes, the length of each electrical pulse employed by the IMP electrode is less than 2 ms, which allows the contractile activities of cells to be immediately captured and recorded while the cells are being paced by IMP electrodes. The optimal conditions for electrical pacing are dependent on the cell type, the inherent beating frequency, and the experimental context. The pacing functionality of the CardioECR system is suitable for both acute pacing regimens to evaluate compound effects on contractility under controlled beating rate and long-term stimulation used for the improvement of functional maturation of hiPSC-CMs.

Raw data collected from IMP electrodes and ECR electrodes were analyzed offline using Agilent xCELLigence RTCA CardioECR data analysis software. The software provides users with more than 25 analysis parameters based on IMP and FP signals to assess cardiac cell beating and electric activities. The fundamental parameter for contractility using cellular impedance measurement are beating amplitude (BAmp) and beating rate (BR). The beating rate is defined as the number of beats per unit of time and is expressed as beats/minute. BAmp is defined as the absolute (delta) Cell Index (CI) value between the lowest and highest points within a beating waveform (Figure 3A). For analysis of FP signal, the FP spike amplitude (FP-Amp) is derived, which is the absolute (delta) value in mV from the lowest point of the initial spike to the highest point of the spike. The FP Duration (FPD) is defined as the period between the negative peak of the FP spike to the maximum or minimum point of the reference wave. The reference wave can be negative or positive depending on how the cells are situated to the FP electrodes (Figure 3B).

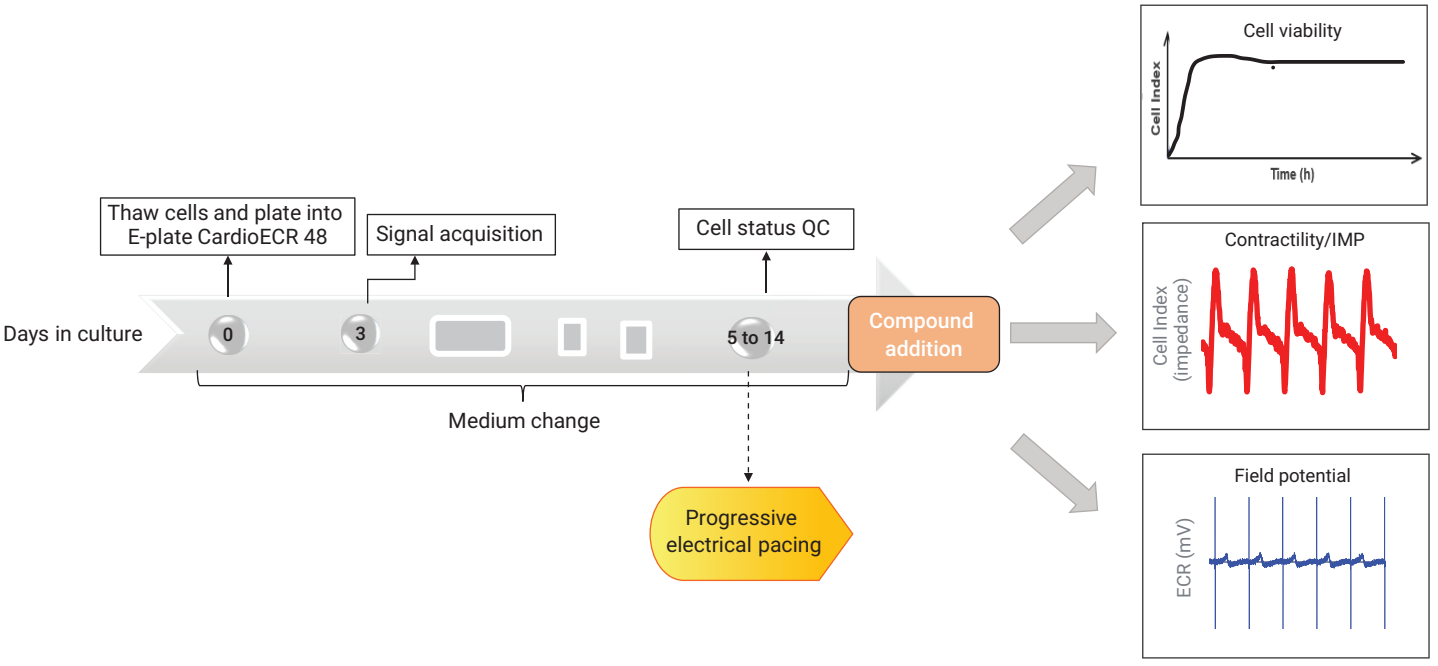

Figure 2. (A) The workflow of hiPSC cardiomyocyte assay using the Agilent xCELLigence RTCA CardioECR system: cell seeding on day 0, start to measure cell performance on day 3, start cell status QC before compound addition, add compounds to the cells if they pass QC. Alternatively, after cells start to generate stable and robust functional activity, approximately 5 days after seeding, progressive electrical pacing is applied to the cells for consecutive 15 days to achieve functional maturation before compound addition.[15] After treatment, cell viability, contraction, and electrophysiology are evaluated via IMP and FP readouts measured by CardioECR system.

Materials and methods

Cell culture

Patient-specific iPSC-derived cardiomyocytes (PS-iPSC CMs) were purchased from FUJIFILM Cellular Dynamics International (FCDI, Madison, WI, USA). The cells were stored in liquid nitrogen until thawed and cultured according to manufacturer instructions. Briefly, each well of the E-Plate CardioECR 48 (Agilent Technologies, Santa Clara, CA, USA) was coated with 50 µL of a 1:100 diluted fibronectin (FN) solution at 10 µg/mL (F1114, Sigma-Aldrich, St. Louis, MO, USA) and incubated at 37 °C for at least 1 hour. Next, the fibronectin solution was replaced with 50 µL of prewarmed iCell cardiomyocyte plating medium. Cells were thawed and diluted in prewarmed plating medium at the manufacture's recommended concentration. 50 µL of the cell suspension was transferred using a multichannel pipette and seeded directly onto a precoated E-Plate CardioECR 48 (20,000 viable and plateable cells/well) in a laminar hood. The plates containing PS-iPSC CMs were kept in the hood at room temperature for 30 minutes, then placed and cultivated in a humidified incubator with 5% CO_2 at 37 °C. The plating medium was replaced with iCell cardiomyocyte maintenance medium 48 hours postseeding. A medium change was performed every other day afterward.

Chemical reagents

All the chemical reagents were purchased from Tocris (Minneapolis, MN, USA), Sigma-Aldrich (St. Louis, MO, USA), or provided by the Chemotherapeutic Agents Repository of the National Cancer Institute. The 1,000-fold chemical stock solutions were prepared in DMSO and stored at −20 °C. The serially diluted chemicals (1,000-fold) were further prepared in DMSO immediately before compound addition. The 10-fold final dilution of the chemicals was prepared with the culture medium for a single-time use only. The final concentration of DMSO in the treated well was 0.1%.

Results and discussion

Evaluation Brugada channelopathy model using CardioECR system

Brugada syndrome (BrS) is one of the more common forms of familial arrhythmic syndromes characterized by a dynamic or persistent ST segment elevation, an enhanced risk of syncope, and sudden cardiac death in young adults without structural heart disease.[7,8] Among several responsible genes identified so far, L-type Ca^{2+} channelopathy of loss-of-function mutations in the CACNA1C (Cav1.2a1) has been reported to give rise to BrS Type 3 (BrS3).[8,9]

This study used BrS3 cardiomyocytes (BrS3 CMs) purchased from Fujifilm CDI (Fujifilm CDI, part number R1136). This BrS3 CM line possesses a change of amino acid 490 from glycine-to-arginine (G490R), which was genetically engineered into the genome of iCell cardiomyocytes (iCell CMs) derived from a healthy donor with no known disease-related genotypes. iCell CMs (Fujifilm CDI, part number R11320) were used as the isogenic control for BrS3 CMs. To investigate the functional consequences of the mutation, the BrS3 CMs and WT iCell CMs were seeded first on the same E-Plate CardioECR 48 at the same seeding density (20,000 cells/well). The cell performance, including attachment, growth, and functional activities were monitored and recorded immediately after cell seeding. Figure 4A shows that BrS3 had slower kinetics of cell attachment and spreading than the control line reflected by the lower slope at the exponential phase of the Cell Index curve. Overall, Cell Index values of BrS3 were generally smaller than the control line. In addition to the attachment and growth profiles, the excitation-contraction profiles of the BrS3 CM and WT iCell CM displayed significant differences. As shown in Figures 4B and 4D, the BAmp of BrS3 CMs was smaller than control cells by 27 ±13% while the BR of BrS3 was faster than the control by 26 ±17%. Even though

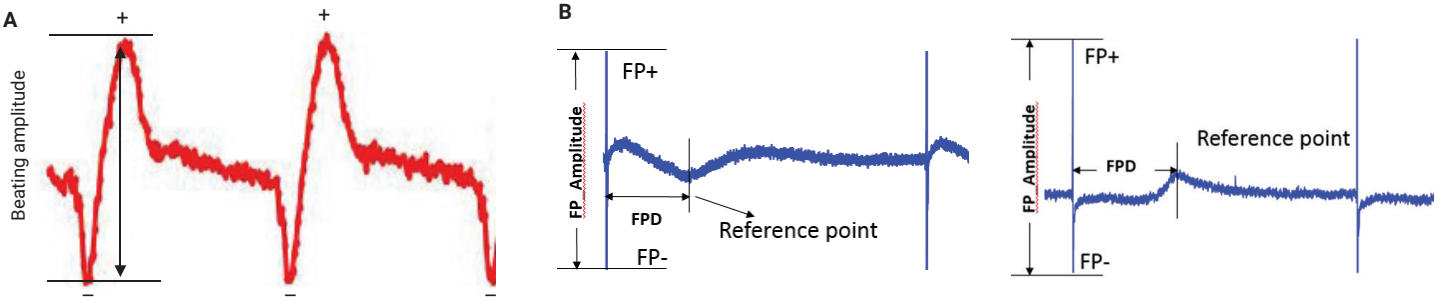

Figure 3. Definition of main parameters used to evaluate cell contractile and field potential activities. (A) The typical IMP waveform/contraction pattern and (B) the typical field potential (FP) waveforms were obtained from diseased and WT CM. The reference point can be negative or positive.

there was no noticeable difference in the Fridericia corrected FPD (FPDc) between the two lines, the BrS3 line exhibited a smaller amplitude of FP spike (FP-Amp) compared to the WT cells.

The next step was to assess the pharmacological responses to the calcium channel modulators, isradipine and BayK 8644. Isradipine is a Ca^{2+} channel blocker with negative inotropic activity. However, BayK 8644 is a Ca^{2+} channel activator, which increases the action potential duration of cardiomyocytes.[10] The cell responses to isradipine and BayK8644 were evaluated by the percentage change in beating amplitude, beating rate, and corrected FPD, 30 minutes postdrug. Isradipine caused a dose-dependent reduction of beating amplitude, increase in beating rate, and decrease in FPDc (Figure 5A) in both lines. BrS3 and WT showed similar percentage changes of the parameters at all tested concentrates. BrS3 and WT cardiomyocytes also had appropriate responses to BayK 8644 as evidenced by a dose-dependent decrease in beating rate and prolongation of FPDc (Figure 5B) due to the activation of the L-type Ca^{2+} channel. However, it appeared that BayK844 caused more significant impacts on beating rate and FPDc in WT than in BrS3. A profound difference in percentage change between BrS3 and WT occurred at concentrations above 10 nM. A concentration of 300 nM BayK 8644 increased FPDc by 77 ±16% in WT and 50 ±9% in BrS3, but decreased beating rate by 40 ±8% in WT and only 15 ±8% in BrS3 (Figure 5B).

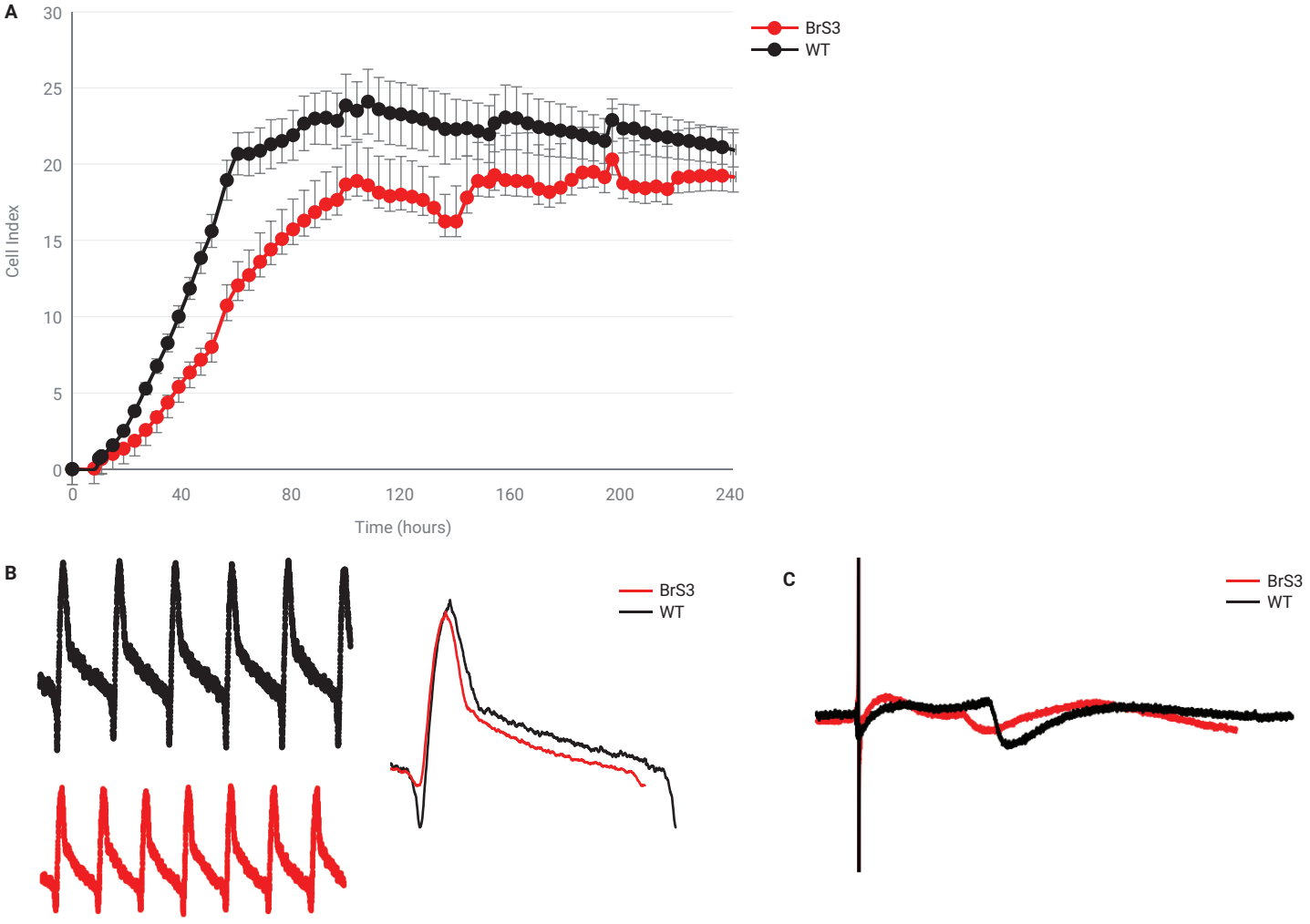

Figures 4A to 4C. The profile of performance obtained from BrS3 and WT CM lines. (A) The overall Cell Index curve was recorded in real time after cell seeding. (B) 10 seconds of IMP waveforms measured in BrS3 (red trace) and WT (black trace) CM lines, which were further averaged into single waveforms shown in the overlay of BrS3 and WT IMP waveforms. (C) The overlay of FP waveforms recorded in BrS3 (red trace) and WT (black trace) CM lines.

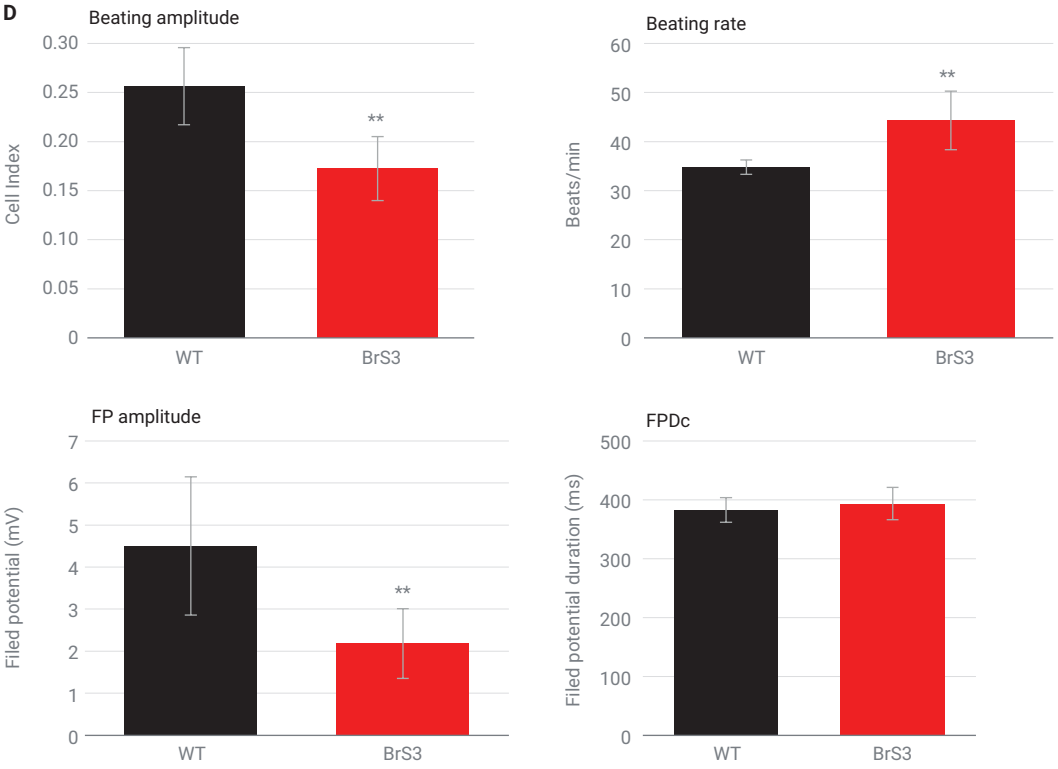

	Br3	WT	% Br3 to WT
BAmp	0.17 ±0.03	0.24 ±0.04	73 ±13%
BR (beats/min)	44 ±6	35 ±1	126 ±17%
FP_Amp (mV)	2.18 ±0.83	4.50 ±1.64	48 ±18%
FPDc (ms)	393.5 ±27.1	382.7 ±21.1	103 ±7%

Figure 4D. The functional activity of BrS3 and WT CM lines were evaluated and compared by beating amplitude (BAmp), beating rate (BR), the amplitude of FP (FP-Amp) and corrected field potential duration (FPDc). The data are represented by mean ±std. dev., N ≥24. Statistical analysis by T-test, ** P <0.05.

Evaluation of LMNA-related dilated cardiomyopathy model using CardioECR system

Dilated cardiomyopathy (DCM) is characterized by weakening heart muscle due to the progressive loss of functional cardiomyocytes, resulting in reduced cardiac output and arrhythmia. A portion of familial DCM is due to mutations in the LMNA gene encoding the nuclear lamina proteins lamin A and C, which have an important role in maintaining the shape and nuclear structure, DNA and protein expression level, and chromatin organization.[11] To get better insights into the pathobiology behind LMNA mutation, the functional phenotype of MyCell Cardiomyocytes DCM (L35P) (Fujifilm CDI, catalog number R1153) was investigated using the CardioECR system. The LMNA-related DCM line (LMNA) was differentiated from patient-specific iPSCs, which harbor the LMNA L35P mutation. In addition, an isogenic control of LMNA-DCM (CTRL) generated using genome engineering strategies to correct the mutation (Fujifilm CDI, catalog number R1154) was used in the study.

As in the BrS3 study, the LMNA and CTRL lines were seeded in the same E-Plate Cardio 48 at the same seeding density (20,000 cells/well). The time course of the overall Cell Index (Figure 6A) showed very similar kinetics between disease and healthy lines. However, the Cell Index curve of the disease line started to show slightly smaller but significant Cell Index values compared to the control after five days post-seeding, which persisted for the rest of the culture time. The functional performance of the control and diseased cells was recorded (Figures 6B and C) and evaluated after both lines reached the stable stage with respect to cell contraction on day 14 in culture. The fundamental contractile activities, namely beating amplitude and beating rate were quantified and evaluated in both lines. LMNA CM exhibited a significantly faster beating rate by 43 ±5% and a smaller beating amplitude by 18 ±8% compared to the

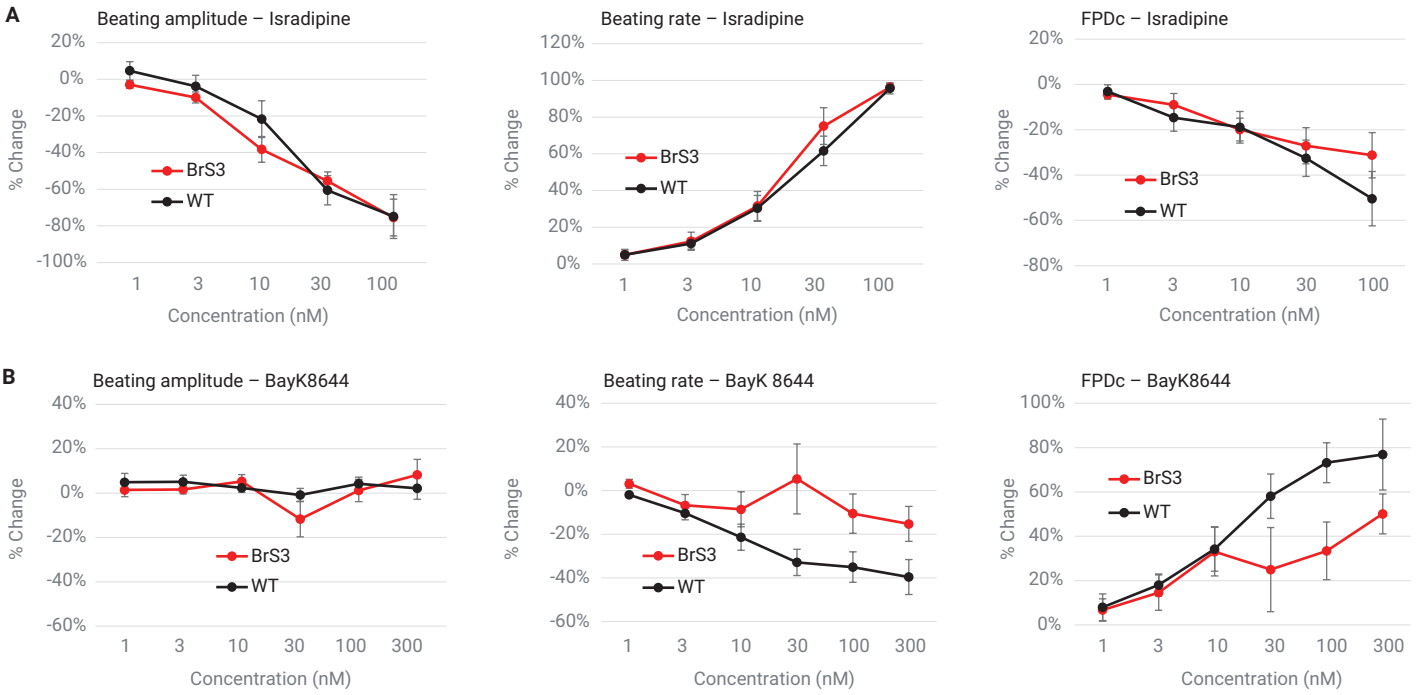

Figure 5. The percentage change of the key parameters after compound addition. (A) % change of beating amplitude, beating rate to the time-matched vehicle CTRL and % change of corrected FPD to the baseline 30 minutes after isradipine addition to BrS3 (red) and WT (black); (B) % change of beating amplitude, beating rate to the time-matched vehicle CTRL and % change of corrected FPD to the baseline 30 minutes after BayK 8644 addition to BrS3 (red) and WT CMs (black).

CTRL (Figure 6D). Due to the profound BR difference observed in both lines, and compared FPD using two approaches, Fridericia's formula and electrical stimulation, which controlled the BR of both lines at 1 Hz during the evaluation of FPD. Interestingly, both approaches showed very similar results. LMNA cells had significantly reduced FPD compared to the control cells (Figure 6D). It has been reported that LMNA-related dilated cardiomyopathy may associate with weakening cardiac contraction.[12] It was further investigated if the LMNA line would show phenotypic and functional differences after the treatment by isoproterenol (ISO), a β adrenergic activator, which increases beating rate and strengthens contractile force *in vivo*. Consistent with previous findings in different hiPSC-CMs[13,14], both lines displayed a significant increase in BR but a decrease in BAmp after ISO addition (Figure 7A). As shown previously[15], the ISO-induced decrease in BAmp was due to the immaturity state of iPSC-derived cardiomyocytes. Therefore, a decision to assess cell responses to ISO after improving the functional maturation of cells using long-term electrical pacing. As demonstrated previously, the control cells displayed a noticeable increase in BAmp by 30% after electrical pacing.[15] Intriguingly, LMNA CM did not have display an improved response to ISO compared to CTLR CM, potentially due to defective contractile functionality of the LMNA line.

This study explored the utility of the CardioECR system for functional assessment of diseased iPSC-CM lines. It first evaluated iPSC-CM that contained a common mutation found in Brugada patients, which is a mutation in the L-type Ca^{2+} channel. Brugada syndrome is a hereditary primary electrical disease, which is associated with right ventricular conduction abnormalities *in vivo*. Even though the conduction property of the BrS3 line in the 2D cell model could not be investigated, there was an observation of abnormal contractile and electrical activities at the cellular level depicted by the simultaneous measurement of IMP readout and FP readout on the CardioECR system. From a contractile/IMP perspective, the BrS3 line exhibited a much smaller beating amplitude and faster beating rate compared to its isogenic control (Figure 4B), which is comparable with the results of hiPSC-CMs treated with L-type Ca^{2+} channel blockers, such as isradipine and nifedipine.[16,17] This finding suggests that the change of amino acid 490 from glycine-to-arginine (G490R) in CACNA1C (Cav1.2a1) is a loss-of-function mutation. It has been reported calcium signaling affects cell-cell adhesion.[18] The slower kinetics of the overall Cell Index (IMP signal) observed in the BrS3 line compared to the control line at the cell attachment phase (Figure 4A) may be related to reduced Ca^{2+} flux induced by the loss-of-function mutation in CACNA1C. In the meantime, the electrophysiologic profile (Figures 4C and 4D) indicated that the BrS3 line did not

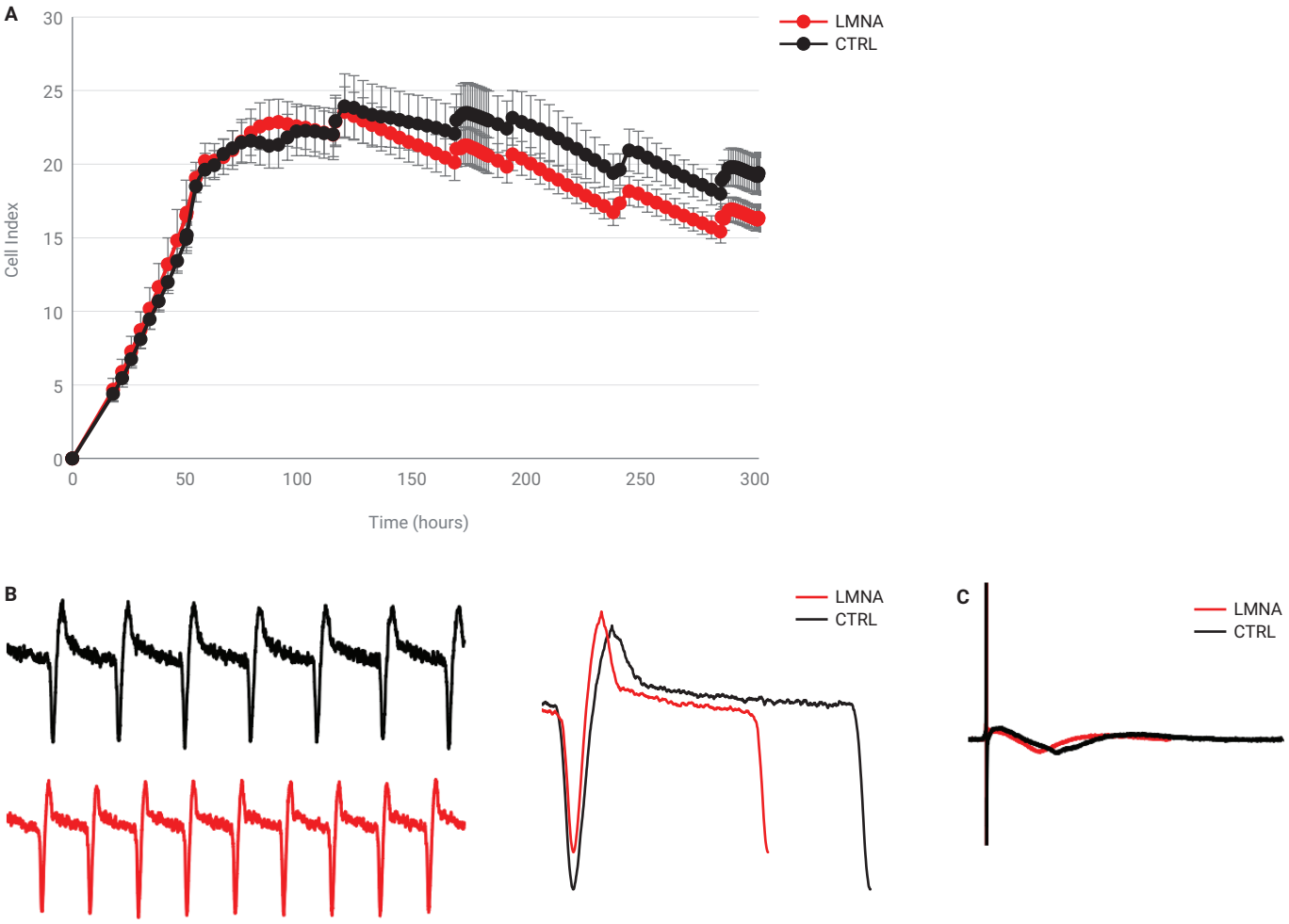

Figure 6A to 6C. The profile of performance obtained from LMNA and CTRL CM lines. (A) The overall Cell Index curve was recorded in real time after cell seeding. (B) 10 seconds of IMP waveforms measured in LMNA (red trace) and CTRL (black trace) CM lines, which were further averaged into single waveforms shown in the overlay of LMNA and CTRL IMP waveforms. (C) The overlay of FP waveforms recorded in LMNA (red trace) and CTRL (black trace) CM lines.

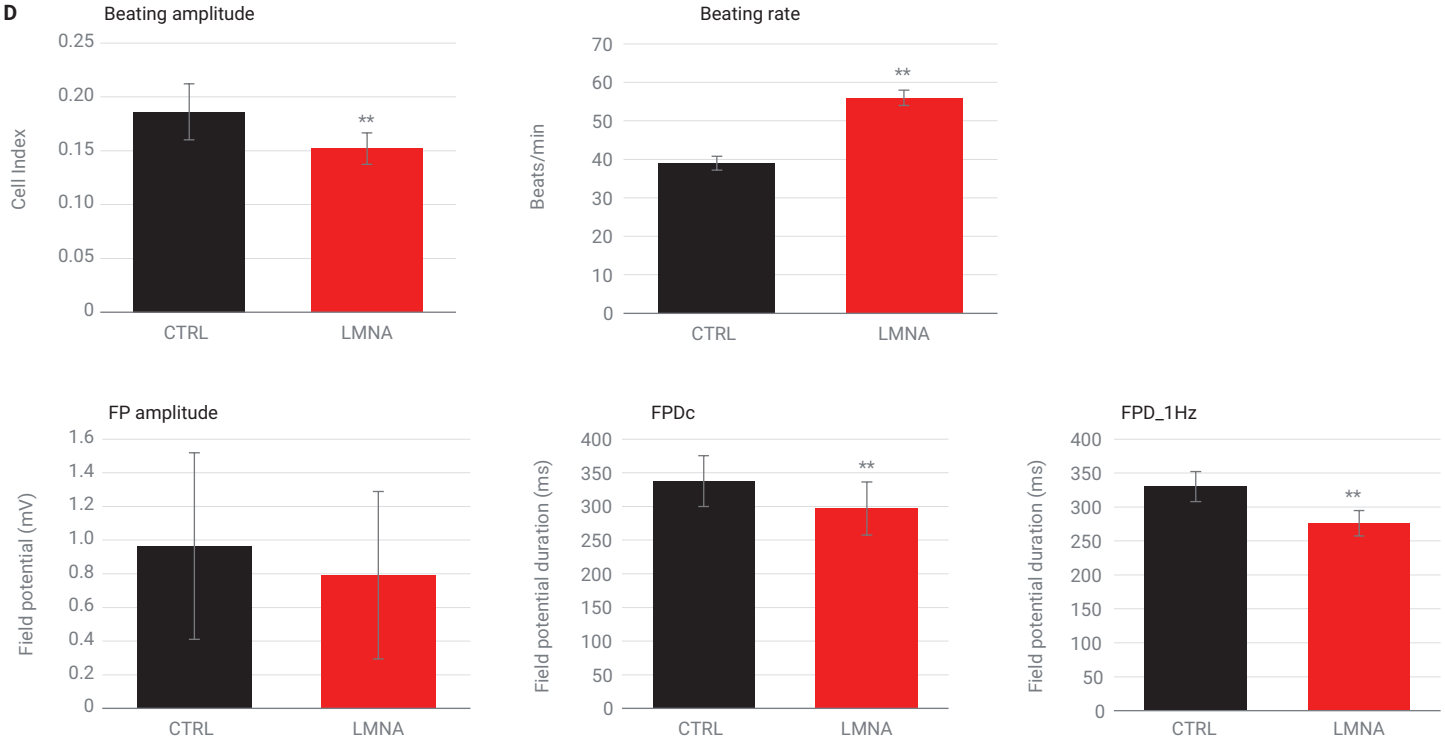

	LMNA	CTRL	% LMNA to CTRL
BAmp	0.15 ±0.02	0.19 ±0.03	82 ±8%
BR (beats/min)	56 ±2	39 ±2	143 ±5%
FP_Amp (mV)	0.79 ±0.50	0.98 ±0.55	82 ±52%
FPDc (ms)	296.9 ±39.5	337.6 ±37.9	88 ±12%
FPD_1Hz	276.1 ±18.9	330.2 ±22.1	84 ±6%

Figure 6D. The functional activity of LMAN and CTRL CM lines were evaluated and compared by BAmp, BR, FP-Amp, FPDc, and FPD that were measured when beating rates of LMNA and CTRL CM lines were controlled at 1 Hz by electrical pacing. The data are represented by mean ±std. dev., N ≥24. Statistical analysis by T-test, ** P <0.05.

Figure 7. Contractile responses of LMNA and CTRL CMs to Isoproterenol (ISO), a known positive inotrope, before (nonpaced) and after electrical pacing (paced). (A) The % change of beating amplitude and beating rate 30 minutes after 100 and 1,000 nM ISO addition to nonpaced LMNA (red bar) and CTRL (black bar) CMs. (B) The % change of beating amplitude and beating rate 30 minutes after 100 and 1,000 nM ISO addition to paced LMNA (red bar) and CTRL (black bar) CMs. The data are represented by mean ±std. dev. (n ≥3).

show a significant difference in FPD after correcting it to the BR using Fridericia's formula. Interestingly, the FP-Amp of the BrS3 line was significantly smaller than the control suggesting the mutation may somehow affect Na^+ channel activity. In addition, the loss-of-function phenotype of BrS3 was also demonstrated by its lower sensitivity to the treatment of BayK8644, the L-type Ca^{2+} channel activator (Figure 5B).

This work extended the study of diseased iPSC CM by evaluating the LMNA line, which was differentiated directly from PS-iPSC derived from a patient that harbors the LMNA L35P mutation. Even though the mutations in the LMNA gene cause a wide range of human diseases, including Hutchinson Gilford Progeria (premature aging syndrome), muscular dystrophy, and familial DCM, LMNA-related familial DCM is primarily characterized by early-onset atrial fibrillation and conduction disorder.[19] Both FP and IMP readouts recorded by the CardioECR system did not show any sign of fibrillation and/or arrhythmic events in the LMNA line throughout the entire culture. However, shorter corrected FPD (Fridericia's formula) in the LMNA line compared to the control was detected. Intriguingly, FPD measured when the BR of LMNA and control cells was synchronized at 1 Hz using electrical pacing of CardioECR showed very similar results to the Fridericia-corrected FPD (Figure 6D), suggesting that Fridericia's formula used *in vivo* is suitable for correcting FPD of spontaneous beating cardiomyocytes in 2D culture. Compared to the control, the baseline profile of LMNA contractility showed much faster BR but smaller BAmp indicating an impaired contraction of LMNA (Figures 6B and 6D). But the extent of contraction force weakening in the LMNA line was not substantial. As reported in the application note of the xCELLigence RTCA ePacer system for maturation[15], long-term electrical pacing improved the contractile property

of hiPSC CMs. Therefore, this study investigated if long-term pacing could have an impact on the phenotypical differences between LMNA and control. The response of control cells to ISO was reversed after 15 days of continuous pacing, as demonstrated by an increase in beating amplitude. However, the response of LMNA to ISO remained the same (Figure 7B) indicating an inherent deficiency in excitation-contraction coupling leading to force generation.

Conclusion

Our data show that the Agilent xCELLigence CardioECR system is well suited to assess the functional differences relating to cell growth and viability, contractility, and electrophysiology of diseased iPSC-CM cells, providing a method to identify unique disease-related phenotypes. Additionally, applying electrical pacing provided yet another approach to delineate phenotypic differences between control and diseased lines. Once a unique disease-associated phenotype is identified, the platform could be used for screening of small molecule as well as genetic manipulation of the cells, which could potentially rescue the cells and, revert to wild type activity.

References

1. Grskovic, M. *et al.* Induced Pluripotent Stem Cells—Opportunities for Disease Modelling and Drug Discovery. *Nat. Rev. Drug Discov.* **2011**, *10*, 915–929.
2. Wu, S. M.; Hochedlinger, K. Harnessing the potential of induced pluripotent stem cells for regenerative medicine. *Nat. Cell Biol.* **2011**, *13*, 497–505.
3. Park, I. H. *et al.* Disease-Specific Induced Pluripotent Stem Cells. *Cell* **2008**,*134*, 877–886.
4. Kiskinis, E.; Eggan, K. Progress Toward the Clinical Application of Patient-Specific Pluripotent Stem Cells. *J. Clin. Investig*. **2010**, *120*, 51–5914.
5. Tiscornia, G. *et al.* Diseases in a Dish: Modeling Human Genetic Disorders Using Induced Pluripotent Cells. *Nat. Med.* **2011**, *17*, 1570–1576
6. Tanaka, A. *et al.*Cardiovascular Disease Modeling Using Patient-Specific Induced Pluripotent Stem Cells, *Int. J. Mol. Sci*. **2015**, *16(8)*, 18894–922.
7. Canpolat, U.; Bayazit, Y.; Aytemir, K. Brugada Syndrome Unmasked by Heat Exhaustion. *Ann. Noninvasive Electrocardiol.* **2017**, *22*.
8. Splawski, I. *et al.* Ca(V)1.2 Calcium Channel Dysfunction Causes a Multisystem Disorder Including Arrhythmia and Autism. *Cell* **2004**, *119*, 19–31.
9. Antzelevitch, C. *et al.* Loss-of-Function Mutations in the Cardiac Calcium Channel Underlie a New Clinical Entity Characterized by ST-Segment Elevation, Short QT Intervals, and Sudden Cardiac Death. *Circulation* **2007**, *115*, 442–449.
10. Thomas, G.; Chung, M.; Cohen, C. J. A Dihydropyridine (Bay k 8644) That Enhances Calcium Currents in Guinea Pig and Calf Myocardial Cells. A New Type of Positive Inotropic Agent. *Circ. Res.***1985**, *56(1)*, 87–96.
11. Goidescu C. M. Dilated Cardiomyopathy Produced by Lamin A/C Gene Mutations *Clujul Med*. **2013**, *86(4)*, 309–312.
12. Luk, A. *et al.* Dilated Cardiomyopathy: a Review. *J. Clin. Pathol.* **2009**, *62*, 219–225.
13. Yang, X.; Pabon, L.; Murry, C. E. Engineering Adolescence: Maturation of Human Pluripotent Stem Cell-Derived Cardiomyocytes. *Circ. Res.* **2014**, *114(3)*, 511–23
14. Ravenscroft, S. M. *et al.* Cardiac Non-myocyte Cells Show Enhanced Pharmacological Function Suggestive of Contractile Maturity in Stem Cell Derived Cardiomyocyte Microtissues. *Toxicol. Sci.* **2016**, *152(1)*, 99–112.
15. Zhang, X.; Li, J.; Abassi, Y. A. Using the Agilent xCELLigence RTCA ePacer for Functional Maturation of Human-Induced Pluripotent Stem Cell-Derived Cardiomyocytes, *Agilent Technologies application note*, publication number 5994-1552EN, **2019**.
16. Abassi, Y. A. *et al.* Dynamic Monitoring of Beating Periodicity of Stem Cell-Derived Cardiomyocytes as a Predictive Tool for Preclinical Safety Assessment. *Br. J. Pharmacol.* **2012**, *165(5)*, 1424–41.
17. Zhang, X. *et al.* Multi-Parametric Assessment of Cardiomyocyte Excitation-Contraction Coupling Using Impedance and Field Potential Recording: A Tool for Cardiac Safety Assessment. *J. Pharmacol. Toxicol. Methods* **2016**, *81*, 201–16.
18. Dalal, P. J.; Muller, W. A.; Sullivan, D. P. Endothelial Cell Calcium Signaling during Barrier Function and Inflammation. *Aging* (Albany NY). **2012** Nov, *4(11)*, 803–822.
19. Siu, C. W. *et al.* Modeling of Lamin A/C Mutation Premature Cardiac Aging Using Patient-Specific Induced Pluripotent Stem Cells. *Aging* (Albany NY) **2012** Nov, *4(11)*, 803–822.

www.agilent.com/chem

For Research Use Only. Not for use in diagnostic procedures.

RA44438.5457523148

This information is subject to change without notice.

Printed in the USA, September 9, 2021
5994-3112EN

Agilent

Trusted Answers